Title
Stretch calculated from grip distance accurately approximates mid-specimen stretch in large elastic arteries in uniaxial tensile tests

Authors
Tian, Lian
Henningsen, Joseph
Salick, Max R
et al.

Publication Date
2015-07-01

DOI
10.1016/j.jmbbm.2015.03.016

Peer reviewed

HHS Public Access

Author manuscript

J Mech Behav Biomed Mater. Author manuscript; available in PMC 2016 July 01.

Published in final edited form as:

J Mech Behav Biomed Mater. 2015 July ; 47: 107–113. doi:10.1016/j.jmbbm.2015.03.016.

Stretch calculated from grip distance accurately approximates mid-specimen stretch in large elastic arteries in uniaxial tensile tests

Lian Tian[1], **Joseph Henningsen**[1], **Max R. Salick**[2], **Wendy C. Crone**[2], **McLean Gunderson**[3], **Seth H. Dailey**[3], and **Naomi C. Chesler**[1,*]

[1]Department of Biomedical Engineering, University of Wisconsin-Madison, Madison, WI 53706-1609, USA

[2]Department of Engineering Physics, University of Wisconsin-Madison, Madison, WI 53706-1609, USA

[3]Department of Surgery, Division of Otolaryngology-Head and Neck Surgery, University of Wisconsin-Madison, Madison, WI 53792-3252, USA

Abstract

The mechanical properties of vascular tissues affect hemodynamics and can alter disease progression. The uniaxial tensile test is a simple and effective method for determining the stress-strain relationship in arterial tissue ex vivo. To enable calculation of strain, stretch can be measured directly with image tracking of markers on the tissue or indirectly from the distance between the grips used to hold the specimen. While the imaging technique is generally considered more accurate, it also requires more analysis, and the grip distance method is more widely used. The purpose of this study is to compare the stretch of the testing specimen calculated from the grip distance method to that obtained from the imaging method for canine descending aortas and large proximal pulmonary arteries. Our results showed a significant difference in stretch between the two methods; however, this difference was consistently less than 2%. Therefore, the grip distance method is an accurate approximation of the stretch in large elastic arteries in the uniaxial tensile test.

Keywords

uniaxial test; stretch estimation; grip distance; imaging technique

*Corresponding author: Naomi C. Chesler, Department of Biomedical Engineering, University of Wisconsin-Madison, 2146 ECB, 1550 Engineering Drive, Madison, WI 53706-1609, USA, chesler@engr.wisc.edu.

Introduction

The mechanical properties of large proximal arteries are of great interest because these arteries strongly impact blood flow in the circulation and heart function (Milnor 1975; Stevens et al., 2012; Wang and Chesler, 2011; Weinberg et al., 2004). Understanding the changes in arterial mechanical properties during cardiovascular disease progression is useful for prognoses and monitoring therapeutic efficacy. Several ex vivo mechanical tests have been used to characterize the mechanical properties of large elastic arteries including uniaxial and biaxial tests, and pressure inflation-force test (Holzapfel, 2006; Kao et al., 2011; Lammers et al., 2008; Sommer et al., 2010; Golob et al., 2015). The uniaxial test is performed with an apparatus that applies a tensile force to a rectangular strip in only one direction. As a result, this test does not mimic the physiological state of the artery, which is loaded three-dimensionally, and cannot fully characterize the anisotropic properties of the artery (Tian and Chesler, 2012; Holzapfel and Ogden, 2009). Despite these limitations, the uniaxial test is often preferred to the other, more physiologically relevant tests due to its simplicity and feasibility when tissue size is limited (Tian and Chesler, 2012; Holzapfel, 2006).

The question of how to accurately measure strain or stretch is important for uniaxial testing of arterial tissue. Many uniaxial test studies use the grip-to-grip distance before and during loading for the stretch calculation (Bulter et al., 1984; Lammers et al., 2008; Tian et al., 2011). Conversely, some studies mark regions of the specimen with visible markers (e.g., ink) prior to testing and obtain the stretch at the mid-section of the specimen by tracking the distances between these markers during the test (Bulter et al., 1984; Holzapfel et al., 2004; Holzapfel 2006; Woo et al., 1983; Zernicke et al., 1984). This latter method, the imaging method, is useful for avoiding or reducing the clamped boundary effect associated with the uniaxial test. However, it requires a significant amount of equipment, software, and calculations, while the determination of mean strain from grip distance is relatively simple. Unfortunately, no experimental studies have verified whether the calculation of strain based on grip distance is an accurate approximation compared to marker motion in the mid-section of tissue specimens from large elastic arteries.

The purpose of this study was to examine if the stretch calculated from grip distance during uniaxial testing on specimens from large elastic arteries is an accurate approximation of the stretch in the middle of the specimen.

Methods

Materials

All experimental studies were performed after approval by the Institutional Animal Care and Use Committee of the University of Wisconsin-Madison and Northwestern University. The large proximal pulmonary arteries and descending aortas were harvested after the euthanasia of the animals from 4 adult canines at Northwestern University and 16 adult canines at the University of Wisconsin-Madison, and stored in PBS at 4°C before dissection and testing.

Mechanical Testing

The aorta and the large proximal pulmonary arteries were prepared for a uniaxial tensile test, less than 24 hours after the euthanasia of animals, with modified experimental protocol of previous studies (Lammers et al., 2008; Tian et al., 2011). Any connective tissue visible on the arteries was removed from the outer wall. This was done carefully and completely to avoid any alterations in the mechanical properties of the vasculature. The pulmonary vasculature was cut with a razor blade into three sections: left pulmonary artery (LPA), right pulmonary artery (RPA), and main pulmonary artery (MPA). Rectangular sections were cut from LPA, RPA, MPA, and aorta in the circumferential direction for testing. Longitudinal rectangular section was also cut from the artery if sufficient longitudinal length remained after the circumferential section was removed. Table 1 summarizes the tissues that were available for testing. Prior to the uniaxial tensile test, the width and thickness of each artery specimen were measured from scaled digital image, and each specimen was marked with black adhesive (Loctite 380 Black Max; Henkel, CT, USA) on the arterial intimal surface for tracking during the testing and for local stretch calculations. Several small markers (>4) were made on the tissue surface within the middle region along the midline of the specimen in the loading direction (Figure 1). All markers on the specimen, with a distance of 1~3 mm between two consecutive ones, were kept as small as possible (0.5~1 mm in diameter) to avoid alteration of the mechanical properties, and they were also kept close to the midline to ensure that they were aligned with the direction of uniaxial loading. The specimen was then clamped by self-aligning grips with sandpaper on each end to avoid specimen slippage. The length between the two grips was measured with digital calipers (with a resolution of 0.5 μm) prior to the test as the reference length (L_0). All tests were done with an Instron 5548 MicroTester tensile testing system (Instron; Norwood, MA, USA), equipped with a 10 N load cell. The MicroTester has a resolution of 0.125 μm and the load cell has a resolution of 10 mN. The tissue specimen was immersed in PBS at 37°C in an environmental chamber throughout the test. Each specimen was first extended by 30% of the initial length which in general won't break the tissue (Lammers et al., 2008) and at a strain rate of 20% gauge length/s which is close to the physiological range (Ingram et al., 1970). The specimen was returned to its initial state before the next test. The specimen was extended again to a higher stretch ratio until the force-extension curve became nonlinear, which indicates collagen engagement (Lammers et al., 2008). The last stretch the specimen was loaded to (without any breakage) was taken as the highest stretch ratio for this specimen. Note that depending on the arterial mechanical properties, different specimens could have different highest stretch ratios. The specimen was then preconditioned at its highest stretch ratio with 10 loading and unloading cycles at a strain rate of 20% gauge length/s. The specimen was finally loaded from the reference state to its highest stretch ratio at a strain rate of 0.2% gauge length/s. During this final loading, images of the specimen were captured once every 10.4 seconds for local stretch calculations and the stretches calculated from grip distance were obtained simultaneously at a sampling rate of 25–50 Hz. Images were captured using a Photometrics MicroPublisher 5.0 RTV and QCapture Pro 5.1.1.14 acquisition software and have a resolution of 0.017 mm/pixel or less. Data for specimens that had fracture, breakage, or slippage were not used.

Calculations

The stretch of the artery during the final loading cycle was calculated in two ways. The ratio of the distance between the grips of the testing systems and the original grip distance was taken as the grip distance stretch:

$$\lambda_{grip}=\frac{L}{L_0}, \quad (1)$$

where L is the length of the specimen between the two grips during loading and L_0 is the original or reference length of the specimen between the two grips before loading. Based on error propagation analysis (Coleman and Steele 1999), the percentage error in stretch due to the instrumentation is $\delta\lambda_{grip}/\lambda_{grip}=\sqrt{\delta_L^2/L^2+\delta_{L_0}^2/L_0^2}$, where δ_L and δ_{L0} are the resolution of L and L_0 measurements, respectively.

The image-based stretch was calculated from the image sequence by tracking the distance between two markers during the test and taking the ratio of that distance and the original distance between these two markers (Figure 1):

$$\lambda_{image}=\frac{l}{l_0}, \quad (2)$$

where l is the distance between two selected markers during loading and l_0 is the original distance between these two markers before loading. Tracking of the markers was done with custom-written MATLAB routines (Digital Image Correlation and Tracking). Briefly, a pair of markers was chosen manually and the MATLAB code could then track this pair of markers in a series of consecutive images and calculate the pixel distance between these two markers for each image. Two to four pairs of markers in the middle region of the same artery specimen were chosen for the stretch calculation and the average stretch of all pairs was reported as the image-based stretch. Note that during image analysis, we physically checked the attachment of the markers to the tissue specimen. In general, the markers were attached well to the tissue specimen. We did not use markers that had slippage during our post-testing examination. Based on error propagation analysis, the percentage error in stretch is $\delta\lambda_{image}/\lambda_{image}=\sqrt{\delta_l^2/l^2+\delta_{l_0}^2/l_0^2}$, where δ_l and δ_{l0} are the resolution of l and l_0 measurements respectively, which are both one pixel, i.e., 0.017 mm.

The difference in stretch between these two methods was calculated as

$$\%=\frac{\lambda_{image}-\lambda_{grip}}{\lambda_{grip}}\times 100. \quad (3)$$

An illustration of the calculation of the difference is shown in Figure 2. For a given grip distance stretch of a specimen, the corresponding time was found from the grip distance stretch-time curve. The image-based stretch was then found from the image-based stretch-time curve at the same instant in time. A series of stretches (1.1–2.2 mm/mm) obtained with the grip distance method (λ_{grip}) were used to determine the time points. The stretches found

with the imaging method (λ_{image}) at each time point were compared to λ_{grip} at the same time point using Eq. (3).

To examine if the difference between the two methods depends on the direction of the samples (circumferential vs. longitudinal directions), the artery site (systemic vs. pulmonary artery) and specimen geometry (specifically the ration of specimen's original length between grips and specimen's original width), we separated the specimens into different groups based on these factors and compared the stretch differences of the two methods between groups. When examining the specimen's length to width ratio (Choi and Horgan, 1977; Jimenez et al., 1989; Noyes et al., 1984; Woo et al., 1983; Woo 1982), we separated the specimens into two groups: group 1 with a ratio of 4:1 or greater and group 2 with a ratio less than 4:1 (Table 1).

Statistical analysis

All results are presented as mean ± SE unless otherwise stated. A z-test was performed on the entire data set of the difference between the grip distance and imaging methods. Bland–Altman analysis (Bland and Altman, 1986) was also used to assess the agreement between these two measurements of stretch on the entire data. Student's t-tests were performed on the specimen groups separated based on direction, tissue site, and geometry. A P-value less than 0.05 was considered statistically significant.

Result

To ascertain the accuracy of our experimental approach, we calculated the error in the stretch from grip distance and imaging methods due to testing system. For grip distance method, the maximum error occurs when the reference length (L_0) is the smallest, which is 5.99 mm, and at the smallest stretch, i.e., 1.1. As a result, the maximum error in percentage in stretch from the grip distance method is 0.0085%. For the imaging method, the maximum error occurs when the original length between the two markers (l_0) is the smallest, which is larger than 2 mm for all the chosen pairs of markers, and also at the smallest stretch, i.e., 1.1. Therefore, the maximum error in percentage in stretch from imaging method is 1.1%, which is several orders of magnitude higher than the error form the grip distance method.

Figure 3 shows the difference in stretch between the grip distance and imaging methods. The mean difference for all grip distance stretch levels from 1.1 to 2.2 mm/mm was less than 1% and positive, ranging from 0.10 ± 0.75% to 0.86 ± 0.33% (Figure 3A). The difference between the two methods was significant ($P < 0.05$) at intermediate grip distance stretches (1.3 to 2.0 mm/mm) but not at the lowest or highest grip distance stretch. Bland-Altman analysis shows good agreement between these two methods on stretch measurement (Figure 3B). The imaging method has a bias of 0.0096 with limits of agreement of 0.099.

We then separated the specimens into two groups based on their geometry: those with a length to width ratio ≥ 4 ($n = 53$) and those with a length to width ratio of < 4 ($n = 52$). The mean differences observed for both groups at all stretches remained below 2% as shown in Figure 4. When the two groups were compared to each other, the differences between the groups were not significant ($P > 0.05$).

Figure 5 shows the difference between the two methods at various grip distance stretches for circumferential and longitudinal directions. The direction of the specimen did not significantly affect the difference between the grip distance stretch and the image-based stretch.

The difference in stretch between the two methods in aorta and proximal pulmonary arteries were consistently less than 2% (Figure 6). At high stretches, the differences between the two types of arteries were not significant.

Discussion

The uniaxial tensile test is an often-used way of characterizing the mechanical properties of soft tissues, and in general, the stretch in the loading direction is estimated using the grip distance. However, the accuracy of this method for estimating stretch and therefore strain is unknown. In this study, by performing the uniaxial tensile test on canine aortas and large proximal pulmonary arteries, we obtained the stretch from the grip distance and from an image acquisition method on the middle section of specimens. We found that the two techniques yield significantly different results, yet this difference was never greater than 2% on average. We also found the difference between these two methods did not depend on the specimen length to width ratio, the specimen direction (circumferential and longitudinal), or the artery site (aorta and pulmonary arteries). The error in stretch due to the accuracy of the testing system is not greater than 0.0085% and 1.1% for grip distance and imaging methods, respectively. We conclude that the experimental system is accurate enough to evaluate the difference between the two methods of estimating stretch.

The stretch estimated from the imaging method should be larger than that calculated from the grip distance because, in uniaxial tensile testing, the stretch is largest at the middle region of a rectangular homogeneous specimen that is far from the grips (Choi and Horgan, 1977; Jimenez et al., 1989; Beer et al., 1992; Gasser et al., 2006; ten Thijie et al., 2007). In addition, theoretical and simulation studies have shown that boundary effects are more significant in anisotropic materials, like arteries, than in isotropic materials (Holzapfel and Ogden, 2009; Zernicke et al., 1984; ten Thijie et al., 2007; Holzapfel 2006; Horgan 1972a,b, 1989; Horgan and Knowles, 1983; Miller and Horgan, 1995; Arridge and Folks, 1976; Waldman and Lee, 2002; Waldman e al., 2002). Boundary effects can be minimized by using a dog-bone shaped specimen and by having a very large gage length to width ratio (Jimenez et al., 1989; Miller and Horgan, 1995). Using the dog bone shape when working with soft tissue is often not feasible due to the likelihood of damage and sometimes limited tissue material. As a result, the length to width ratio of our specimens varied from 1.6 to 8.6. Nevertheless, we found that the difference in the stretch between the two methods was less than 2% on average. This suggests that the variation in strain from the center region to the boundaries is small in these tissues for the strain range tested here. In addition, when the different specimens were separated into two groups by the length to width ratio of 4, no significant differences in the difference of stretch between the two methods were seen, although the group with the length to width ratio larger than 4 (group 1) showed slightly larger differences in general. Note that some experimental studies found smaller strain from imaging method, which is probably due to specimen slippage, drying or geometry variation

(e.g., Butler et al., 1984; Zernicke et al., 1984). This study does not include data with these changes in specimen and the conclusion from this study is not applicable to those conditions.

At high stretches of 2.1 and 2.2 there are slightly larger differences between the two methods than at lower stretches. One reason could be that there are fewer data points at these high stretches. At stretches of 2.1 and 2.2, there were 36 and 21 data points, respectively, whereas at lower stretches there are more than 61 data points. Another reason could be a small amount of marker slippage or change in marker orientation at high stretch.

Studies have indicated that a difference in the modulus of different directions, or the degree of anisotropy, also affects the stretch distribution along the loading direction (Holzapfel and Ogden, 2009; Choi and Horgan, 1977; Zernicke et al., 1984; Beer et al., 1992; ten Thije et al., 2007; Holzapfel 2006; Horgan 1972a, b, 1989; Horgan and Knowles, 1983; Miller and Horgan, 1995). In general, the circumferential direction is stiffer than the longitudinal direction for both aorta and large pulmonary arterial tissue. Also, the aorta is stiffer than the large proximal pulmonary arteries in both directions (Miller 1975; Vaishnav and Vossoughi, 1987). When specimens were separated based on the direction of the specimen (i.e., circumferential and longitudinal directions) or the artery site (aorta and pulmonary arteries), the stretch differences were never significant. Nevertheless, the degree of anisotropy of these arterial specimens may not be too much different from each other. Without knowledge of the degree of anisotropy of these arterial specimens, it is not known whether the current result can be applied to other tissues with different degrees of anisotropy.

Tissues were loaded to a stretch higher than the collagen fiber engagement range. As a result, the tested stretch range in general covers the physiological stretch range in both healthy and diseased conditions (Schulze-Bauer and Holzapfel, 2003; Tian et al., 2012; Zeinali-Davarani et al., 2013; Tian et al., 2014). Moreover, 2 out of 16 animals developed mild pulmonary hypertension and our data did not find significant differences between these 2 animals and the others regarding the difference in stretch estimation between the two methods. Therefore, the result, i.e., the 2% difference between the two methods, is applicable in the physiological stretch ranges in both healthy and diseased conditions.

Whereas the stretch range used in this study is physiological, the stretch rate is subphysiological. We preconditioned tissues with a physiological stretch rate, but during data collection we used a lower frequency due to the camera's low image capture rate (maximum 1 frame per 1.4 s to obtain image with a resolution of 0.017 mm/pixel or less). Nevertheless, at higher stretch rate (20% gage length/s), the local stretch rate throughout the specimen would likely increase in proportion to that measured at low stretch rate (0.2% gage length/s). If this is the case, the results of this study will be also applicable under higher strain rate, i.e., physiological strain rate testing. However, we did not perform physiological strain rate testing, which would have allowed us to obtain data for the two methods simultaneously. Whether our conclusions remain valid at a higher, more physiological strain rate awaits confirmation.

Some additional limitations are noted in this study. First, we were limited by the size of each artery and could not get both circumferential and longitudinal specimens from each canine

artery. Second, a clamped boundary was used in this study. It is unclear whether the present results can be applied to cases with suture boundaries, which is also a common attachment method for the uniaxial test. Third, a rectangular section cut from an artery, whether in the circumferential or longitudinal direction, is not truly planar, which introduces error in the calculations. The specimens, especially the circumferential specimens, were curved at their zero stress state (Tian et al., 2011; Vaishnav and Vossoughi, 1987). Any stresses on specimen caused by loading it in a planar orientation were not taken into account.

In summary, the difference in stretch calculation between the grip distance method and the imaging method was statistically significant, but sufficiently small and independent of the tissue site, specimen direction or length to width ratio of the specimen. We conclude that the grip distance method is a good approximation for the stretch estimation in the uniaxial tensile testing of large elastic arteries.

Acknowledgments

This study was supported in part by National Institutes of Health (NIH) grants R01-HL105598 (NCC) and the funding support from Department of Surgery (SHD) at the University of Wisconsin-Madison. The authors gratefully thank Dr. Rishi Arora from Northwestern University for sharing with us canine tissues. The authors would like to thank Mr. Graham Fischer and Mr. Andrew Glaudell from the Department of Engineering Physics at the University of Wisconsin-Madison for assistance in performing mechanical testing on arterial tissues. Mr. Chandler Benjamin from the Department of Engineering Physics at the University of Wisconsin-Madison is also acknowledged for help in characterizing the camera capture rate.

References

Arridge RGC, Folkes MJ. Effect of sample geometry on the measurement of mechanical properties of anisotropic materials. Polymer. 1976; 17:495–500.

Beer, FP.; Johnston, ER.; Dewolf, JT. Mechanics of Materials. New York: MacGraw-Hill; 1992.

Bland JM, Altman DG. Statistical methods for assessing agreement between two methods of clinical measurement. Lancet. 1986; 1:307–310. [PubMed: 2868172]

Butler DL, Grood ES, Noyes FR, Zernicke RF, Brackett K. Effects of structure and strain measurement technique on the material properties of young human tendons and fascia. J Biomech. 1984; 17:579–596. [PubMed: 6490671]

Choi I, Horgan CO. Saint-Venant's principle and end effects in anisotropic elasticity. J Appl Mech. 1977; 44:424–430.

Coleman, HW.; Steele, WG. Experimentation and Uncertainty Analysis for Engineers. New York: Wiley; 1999.

Gasser TC, Ogden RW, Holzapfel GA. Hyperelastic modelling of arterial layers with distributed collagen fibre orientations. J R Soc Interface. 2006; 22:15–35. [PubMed: 16849214]

Golob MJ, Tian L, Wang Z, Zimmerman TA, Caneba CA, Hacker TA, Song G, Chesler NC. Mitochondria DNA mutations cause sex-dependent development of hypertension and alterations in cardiovascular function. J Biomech. 2015; 48:405–412. [PubMed: 25582357]

Holzapfel GA. Determination of material models for arterial walls from uniaxial extension tests and histological structure. J Theor Biol. 2006; 238:290–302. [PubMed: 16043190]

Holzapfel GA, Sommer G, Regitnig P. Anisotropic mechanical properties of tissue components in human atherosclerotic plaques. J Biomech Eng. 2004; 126:657–665. [PubMed: 15648819]

Holzapfel GA, Ogden RW. On planar biaxial tests for anisotropic nonlinearly elastic solids. A continuum mechanical framework. Math Mech Solids. 2009; 14:474–489.

Horgan CO. Some remarks on Saint-Venant's principle for transversely isotropic composites. J Elasticity. 1972a; 2:335–339.

Horgan CO. On Saint-Venant's principle in plane anisotropic elasticity. J Elasticity. 1972b; 2:169–180.

Horgan CO. Recent developments concerning Saint-Venant's principle: An update. Appl Mech Rev. 1989; 42:295–303.

Horgan CO, Knowles JK. Recent developments concerning Saint-Venant's principle. Adv Appl Mech. 1983; 23:179–269.

Ingram RH, Szidon JP, Fishman AP. Response of the main pulmonary artery of dogs to neuronally released versus blood-borne norepinephrine. Circ Res. 1970; 26(2):249–262. [PubMed: 5412538]

Jimenez ML, Brown TD, Brand RA. The effects of grip proximity on perceived local in vitro tendon strain. J Biomech. 1989; 22:949–955. [PubMed: 2613729]

Kao PH, Lammers SR, Tian L, Hunter K, Stenmark KR, Shandas R, Qi HJ. A microstructurally driven model for pulmonary artery tissue. J Biomech Eng. 2011; 133:051002. [PubMed: 21599093]

Lammers SR, Kao PH, Qi HJ, Hunter K, Lanning C, Albietz J, Hofmeister S, Mecham R, Stenmark KR, Shandas R. Changes in the structure-function relationship of elastin and its impact on the proximal pulmonary arterial mechanics of hypertensive calves. Am J Physiol Heart Circ Physiol. 2008; 295:H1451–H1459. [PubMed: 18660454]

Miller KL, Horgan CO. End effects for plane deformations of an elastic anisotropic semi-infinite strip. J Elasticity. 1995; 38:261–316.

Milnor WR. Arterial impedance as ventricular afterload. Circ Res. 1975; 36:565–570. [PubMed: 1122568]

Noyes FR, Butler DL, Grood ES, Zernicke RF, Hefzy MS. Biomechanical analysis of human ligament grafts used in knee-ligament repairs and reconstructions. J Bone Joint Surg Am. 1984; 66:344–352. [PubMed: 6699049]

Schulze-Bauer CAJ, Holzapfel GA. Determination of constitutive equations for human arteries from clinical data. J Biomech. 2003; 36:165–169. [PubMed: 12547353]

Sommer G, Regitnig P, Koltringer L, Holzapfle GA. Biaxial mechanical properties of intact and layer-dissected human carotid arteries at physiological and supraphysiological loadings. Am J Physiol Heart Circ Physiol. 2010; 298:H898–H912. [PubMed: 20035029]

Stevens GR, Garcia-Alvarez A, Sahni S, Garcia MJ, Fuster V, Sanz J. RV dysfunction in pulmonary hypertension is independently related to pulmonary artery stiffness. JACC Cardiovasc Imaging. 2012; 5:378–387. [PubMed: 22498327]

ten Thije R, Akkerman R, Huétink J. Large deformation simulation of anisotropic material using an updated lagrangian finite element method. Comput Method Appl M. 2007; 196:3141–3150.

Tian L, Chesler NC. In vivo and in vitro measurements of pulmonary arterial stiffness: A brief review. Pulm Circ. 2012; 2:505–517. [PubMed: 23372936]

Tian L, Lammers SR, Kao PH, Reusser M, Stenmark KR, Hunter KS, Qi HJ, Shandas R. Linked opening angle and histological and mechanical aspects of the proximal pulmonary arteries of healthy and pulmonary hypertensive rats and calves. Am J Physiol Heart Circ Physiol. 2011; 301:H1810–H1818. [PubMed: 21856906]

Tian L, Lammers SR, Kao PH, Albietz JA, Stenmark KR, Qi HJ, Shandas R, Hunter KS. Impact of residual stretch and remodeling on collagen engagement in healthy and pulmonary hypertensive calf pulmonary arteries at physiological pressures. Ann Biomed Eng. 2012; 40:1419–1433. [PubMed: 22237861]

Vaishnav RN, Vossoughi J. Residual stress and strain in aortic segments. J Biomech. 1987; 20:235–239. [PubMed: 3584149]

Waldman SD, Lee JM. Boundary conditions during biaxial testing of planar connective tissues. Part 1: Dynamic behavior. J Mater Sci: Mater Med. 2002; 13:933–938. [PubMed: 15348186]

Waldman SD, Sacks MS, Lee JM. Boundary conditions during biaxial testing of planar connective tissues. Part II: Fiber orientation. J Mater Sci Lett. 2002; 21:1215–1221.

Wang Z, Chesler NC. Pulmonary vascular wall stiffness: An important contributor to the increased right ventricular afterload with pulmonary hypertension. Pulm Circ. 2011; 1:212–223. [PubMed: 22034607]

Weinberg CE, Hertzberg JR, Ivy DD, Kirby KS, Chan KC, Valdes-Cruz L, Shandas R. Extraction of pulmonary vascular compliance, pulmonary vascular resistance, and right ventricular work from

single-pressure and Doppler flow measurements in children with pulmonary hypertension: A new method for evaluating reactivity in vitro and clinical studies. Circulation. 2004; 110:2609–2617. [PubMed: 15492299]

Woo SL. Mechanical properties of tendons and ligaments. I Quasi-static and nonlinear viscoelastic properties. Biorheology. 1982; 19:385–396. [PubMed: 7104480]

Woo S, Gomez MA, Seguchi Y, Endo CM, Akeson WH. Measurement of mechanical properties of ligament substance from a bone-ligament-bone preparation. J Orthop Res. 1983; 1:22–29. [PubMed: 6679572]

Zeinali-Davarani S, Chow MJ, Turcotte R, Zhang Y. Characterization of biaxial mechanical behavior of porcine aorta under gradual elastin degradation. Ann Biomed Eng. 2013; 41:1528–1538. [PubMed: 23297000]

Zernicke RF, Butler DL, Grood ES, Hefzy MS. Strain topography of human tendon and fascia. J Biomech Eng. 1984; 106:177–180. [PubMed: 6738023]

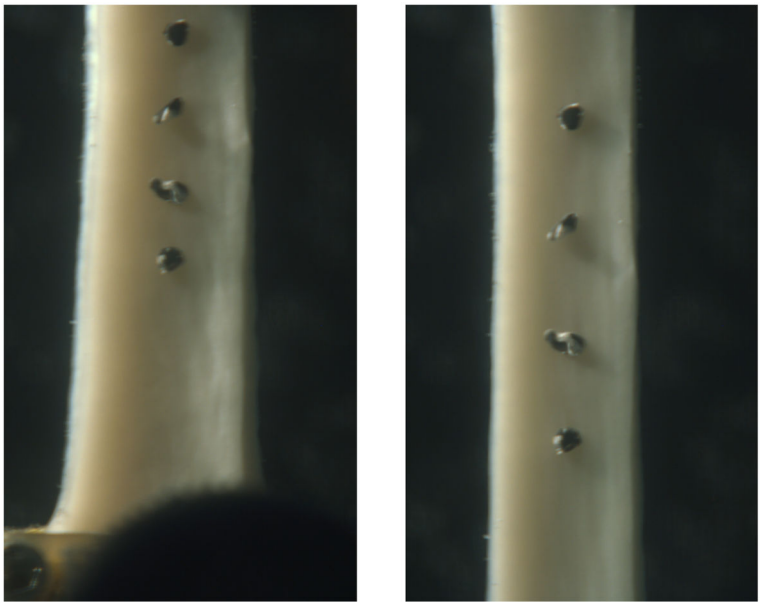

Figure 1.

Sample images of the test specimen after being marked with black adhesive. The distance between markers at the initial length (left) was compared to the distance between the same two markers at a later time point (right) to calculate the stretch. In this example, if we label these four markers as 1, 2, 3 and 4, we have three pairs (i.e., pairs 1 and 2, 2 and 3, and 3 and 4) for the displacement measurement in the imaging method.

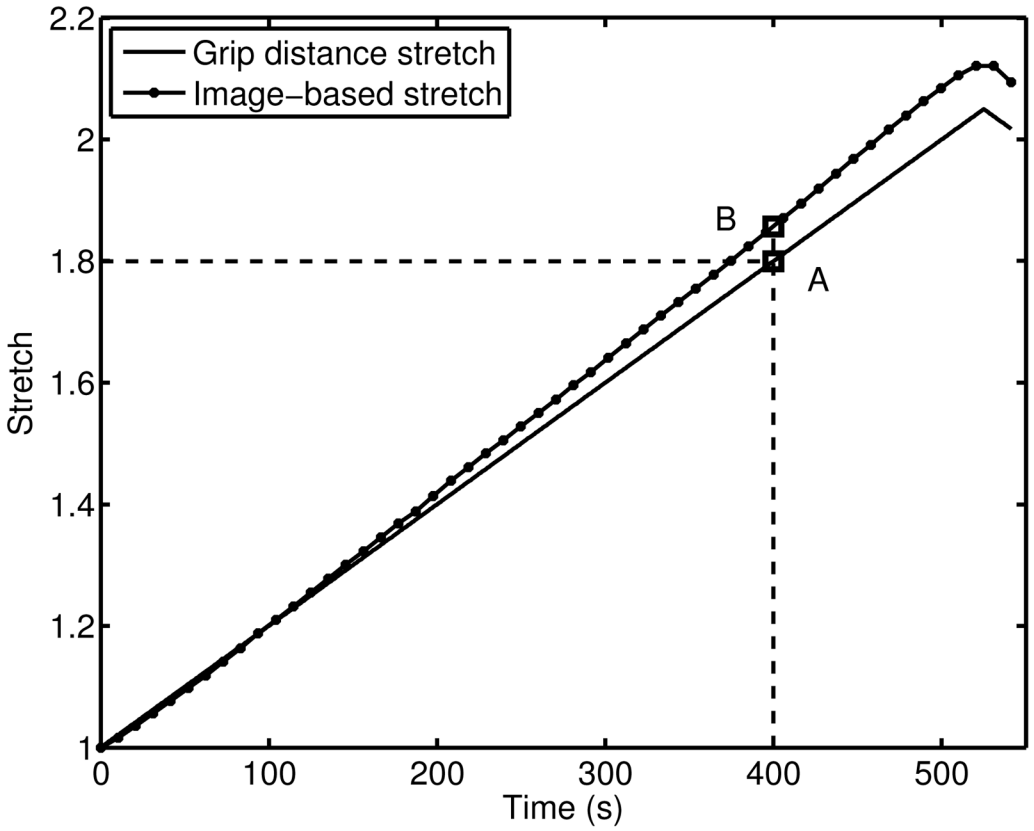

Figure 2.

Illustration of how the stretches were found from each method to be used in the difference calculation seen in Eq. (3). For a given grip distance stretch (1.8 in this illustration), we first found the corresponding time (at 400 s) from the grip distance stretch-time curve (See point A with square symbol). We then found the imaged-based stretch from the imaged-based stretch-time curve at this time (see point B with square symbol which is above point A).

(A)

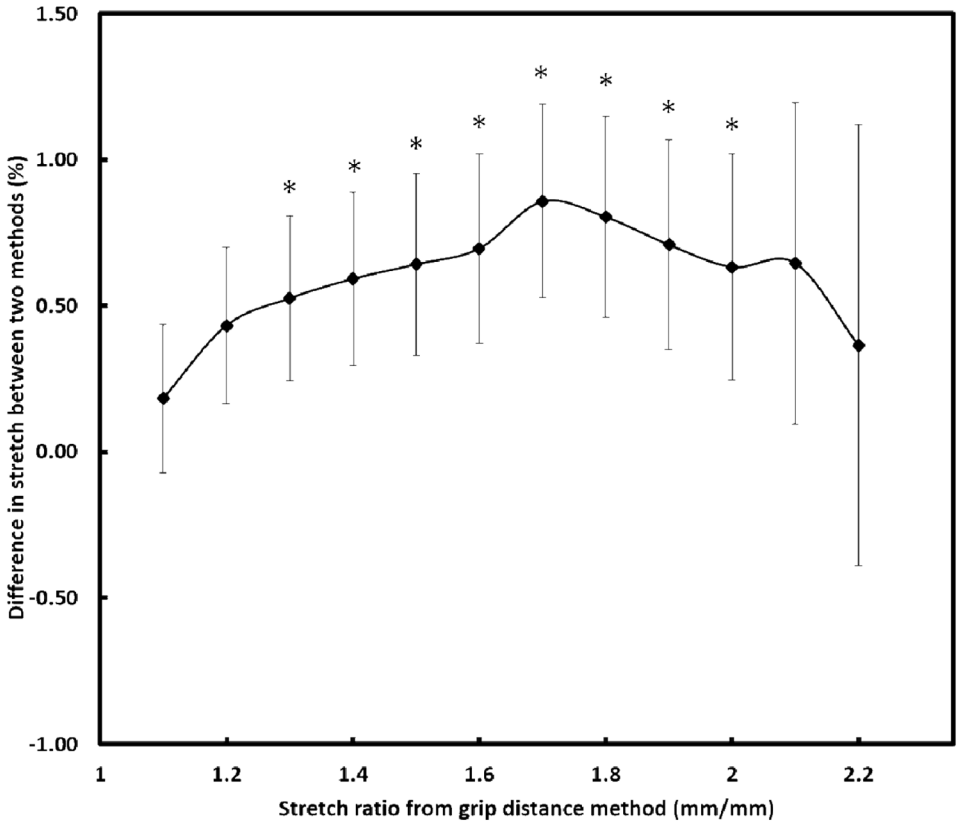

(B)

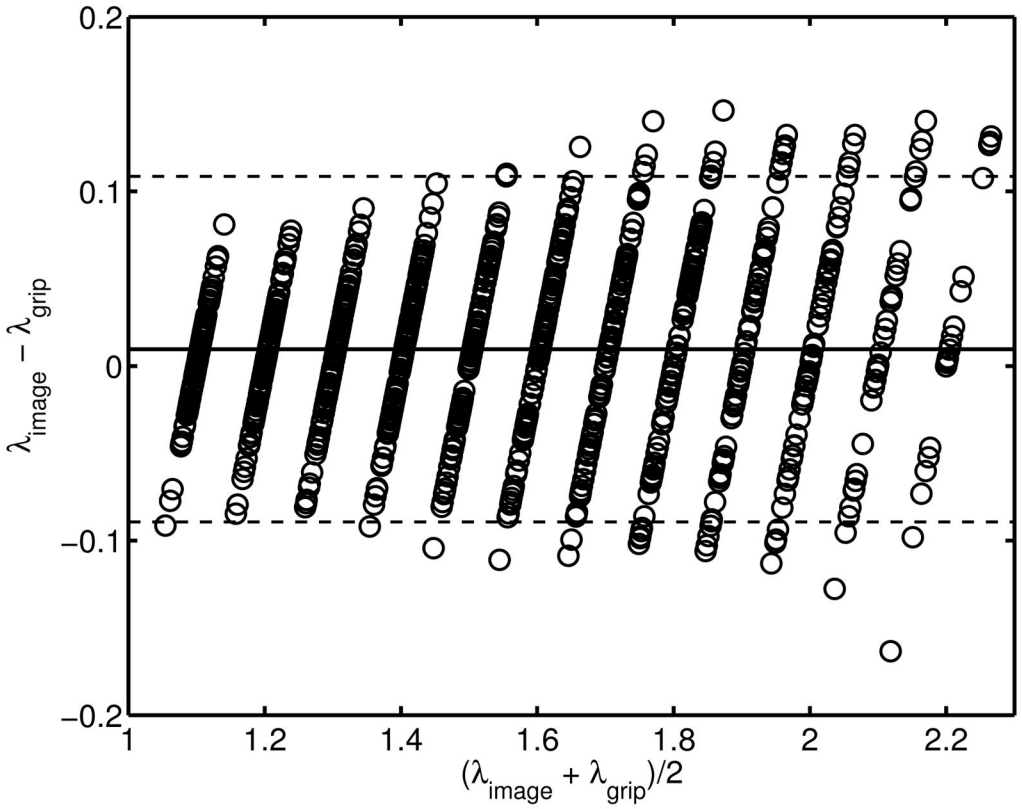

Figure 3.

A. Percent difference in stretch between the two methods as a function of grip distance stretch. *, $P < 0.05$ for the difference compared to zero. B. Bland–Altman agreement analysis between the two measurements of stretch.

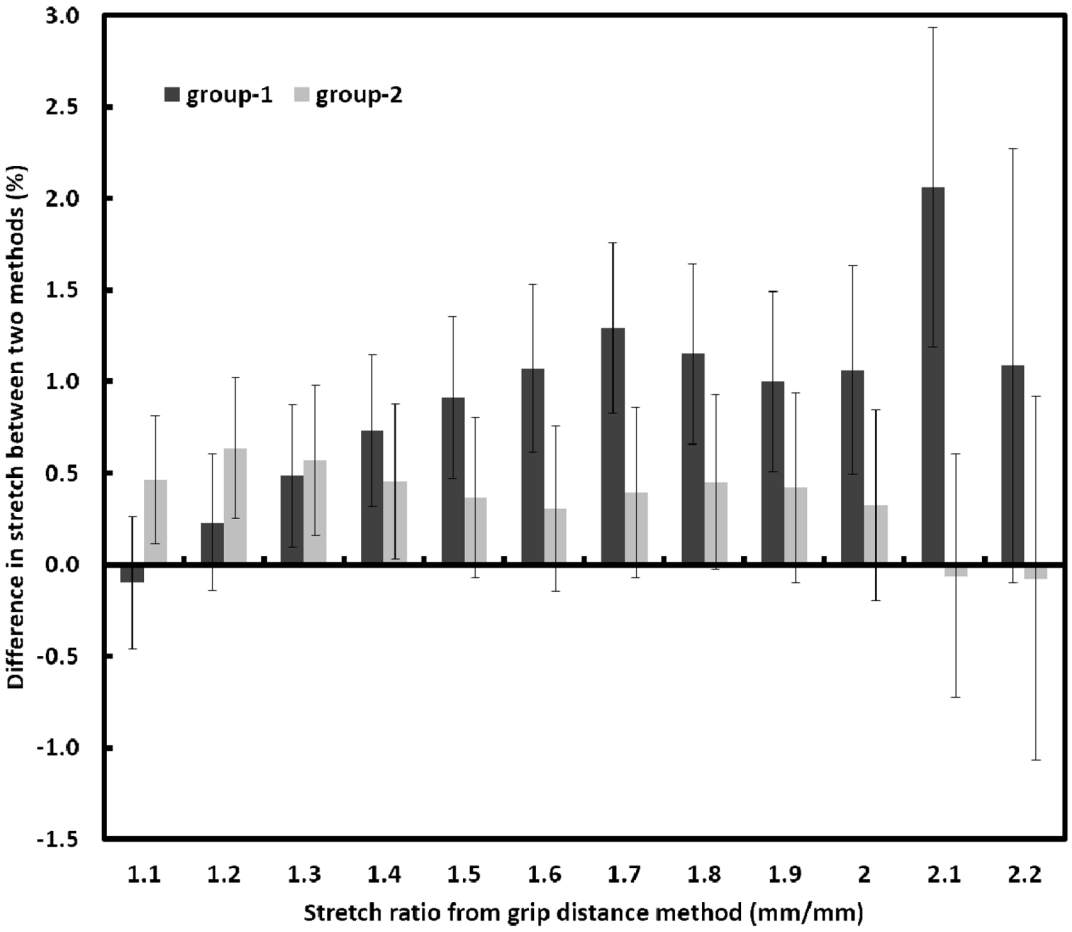

Figure 4.

Percent difference in stretch between the two methods as a function of grip distance stretch for specimens separated based on their geometry. Group-1 consisted of specimens with a gage length to width ratio ≥ 4 and Group-2 consisted of specimens with a gage length to width ratio of < 4.

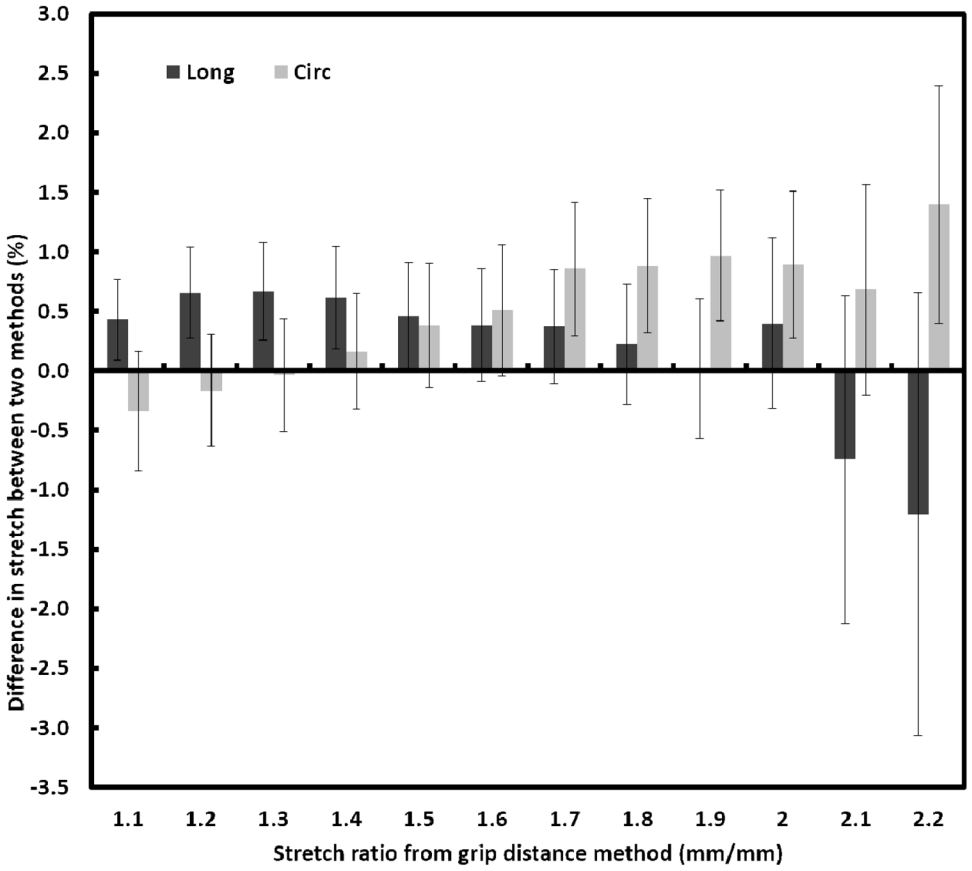

Figure 5.

Percent difference in stretch between the two methods as a function of grip distance stretch for specimens in both the longitudinal (Long) and circumferential (Circ) directions.

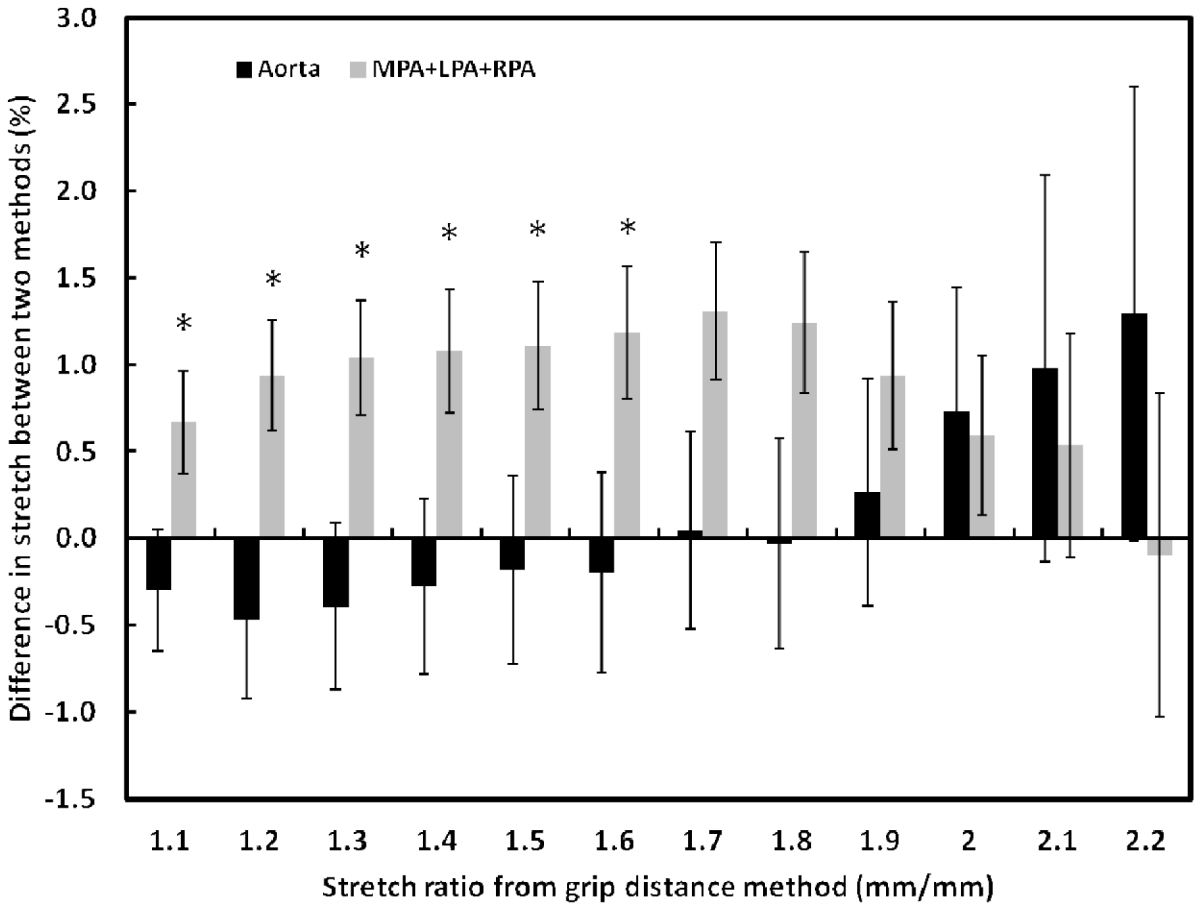

Figure 6.

Percent difference in stretch between the two methods as a function of grip distance stretch for specimens in both aorta and the different large proximal pulmonary arteries. LPA, left pulmonary artery; RPA, right pulmonary artery; MPA, main pulmonary artery. *, $P < 0.05$ between the two groups.

Table 1

Summary of the number and geometry of specimens prepared for testing according to type of tissue and direction of specimen.

	Circumferential				Longitudinal			
Tissue	**N**	**N1**	***L* (mm)**	***L*/*W***	**N**	**N1**	***L* (mm)**	***L*/*W***
AO	19	7	14.5±3.6	3.9±1.0	19	14	22.7±5.0	4.4±1.1
MPA	17	16	18.6±2.8	5.7±1.4	N/A			
LPA	17	5	10.6±2.1	3.5±0.9	5	0	10.3±2.2	2.8±0.7
RPA	17	9	12.7±1.6	4.1±0.9	12	2	11.1±2.7	3.2±1.0

AO, aorta; MPA, main pulmonary artery; LPA, left pulmonary artery; RPA, right pulmonary artery; N, number of specimens; *L*, gage length of specimen during the uniaxial test; *W*, specimen width; N1, the number of specimens within group-1 ($L/W \geq 4$), and the rest specimens are categorized as Group-2. A threshold of 4 for L/W was chosen based on the literature (see text).